Thermodynamic properties of the Δ-chain model in a uniform magnetic field

Hiromi Otsuka
Department of Physics, Tokyo Metropolitan University, Hachioji, Tokyo, 192-03, Japan
(Received 15 June 1994)

A numerical approach for calculating an eigenvalue distribution function is developed and it is applied to the study on a fully frustrated spin system called the Δ-chain model. We examine the magnetic-field dependence of the specific heat to clarify the relationship between the highly frustrated spins and the lower-temperature peak which has been extensively investigated by Kubo. Our numerical data show that with the increase of magnetic field, the peak width becomes broader and the height lower. This sensitive dependence should be caused by lowering the high degeneracy of states contributing to the peak formation. On the other hand, we also find that the higher-temperature peak observed commonly in antiferromagnetic quantum spin chains is almost unchanged.

I. INTRODUCTION

So far, the frustrated spin systems have been treated extensively in both experimental and theoretical investigations. Among them, in particular, the quantum Heisenberg antiferromagnets on the *kagomé* lattice with nearest-neighbor coupling have recently attracted much interest. This is partly because the system is thought to be a plausible model for the second layer ^{3}He system ($S=\frac{1}{2}$) adsorbed on graphite whose experimental data for the heat capacity show a double peak anomaly;[1] it is also the theoretical model of the compounds such as $SrCr_8Ca_4O_{19}$ ($S=\frac{3}{2}$).[2] From a theoretical view point, the system is a widely known example of a so-called "fully frustrated quantum spin system" and thus the classical ground state has infinite continuous degeneracy by its definition. A simple picture predicts that the classical Heisenberg antiferromagnet on the *kagomé* lattice has a residual entropy per site, which is contributed from the following two sources: (i) The first is the number of configurations where each spin is pointing to one of the three directions ($\mathcal{A}$, $\mathcal{B}$, $\mathcal{C}$, which take $2\pi/3$ rad with each other) with two nearest-neighboring spins not pointing to a same direction (we assume that the system becomes coplanar).[3] It is thus equal to the degeneracy of the ground states of the antiferromagnetic three-state Potts model. (ii) Starting from one of the above possible configurations, one can recognize another source: the ground-state energy is not changed by the continuous local rotation of the spins on every closed loop consisting of, e.g., $\mathcal{B}$ and $\mathcal{C}$ spins around the axis defined by $\mathcal{A}$. Harris, Kallin, and Berlinsky have studied the quantum antiferromagnet by using linear spin-wave theory and clarified that this continuous degeneracy gives rise to a dispersionless mode.[4] Consequently, the assumed order is unstable within the semiclassical treatment, because of (ii).

In such a condition, the quantum effects can play a definitely important role in determining the basic properties such as the type of magnetic order, which may be unusual for the magnets without frustrations. For example, as was discussed by Sachdev using the large-N expansion method,[5] the classical ordered state (a $\sqrt{3}\times\sqrt{3}$ structure) is selected from the large number of possible candidates by quantum effects for large S. On the other hand, when S becomes small, the quantum disordered ground state might be realized due to both the large quantum fluctuations and the effects of the lattice with a small coordination number. Nevertheless, there is no established conclusion whether the ground state is ordered or disordered, which remains a greatly challenging problem.

In this paper, we will study the one-dimensional (1D) $S=\frac{1}{2}$ system called a Δ-chain model, which is also a fully frustrated quantum spin system and the relation with the *kagomé* lattice is shown in Fig. 1. There are some previous works on this model and rigorous results have been obtained for the ground state.[6–9] However, as was discussed by Kubo, the ground state of the system with the periodic boundary condition is a twofold degenerate dimer state; thus, the finite excitation gap exists, which is basically the same as that of the Majumdar-Ghosh model.[10] As a result, the excited states or the finite-temperature properties should be investigated to learn the essence of full frustration effects.

The quantum Monte Carlo simulation method is one of the powerful techniques in the numerical methods, but the negative sign problem may become severe when we apply it to quantum spin systems with frustrations.[11] It is

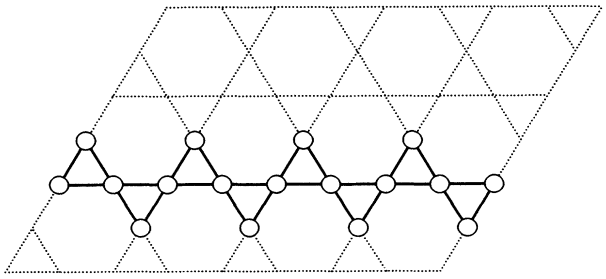

FIG. 1. The Δ-chain model defined on the *kagomé* lattice (dotted line). The solid lines represent the antiferromagnetic exchange coupling and the spins are located on the sites (open circles).

thus probably hard to get reliable results. Another available standard approach is the exact diagonalization method: when the ground state and a few excited states are of interest, we may use the Lanczos procedure, which requires the memory size of order $\mathcal{N}$ for a $\mathcal{N}$-dimensional Hamiltonian matrix. However, full diagonalization should be carried out to clarify the finite-temperature properties exactly, which needs $O(\mathcal{N}^2)$ memory; the manageable system size then becomes rather small comparing with the former case.

Our purpose of this paper is twofold: first, we present and investigate a method to evaluate the eigenvalue distribution function of a large scale matrix, where $O(\mathcal{N})$ memory is required. As the implementation of the method, we employ a random vector sampling technique which is similar to the idea presented by Imada and Takahashi in *the quantum transfer Monte Carlo method.*[12] In our formulation, the distribution function is expressed as the averaged value of the imaginary part of the Green's-function matrix element, which is accurately evaluated by the use of *the recursion method.*[13–15] As a second aim, we explore the thermodynamic properties of the Δ-chain model by using the evaluated eigenvalue distribution function. The double peak structure of the specific heat is discussed: the lower-temperature peak position and its height are estimated more accurately than those obtained by the transfer-matrix method in Ref. 6. Moreover, the simulations are also carried out to clarify the magnetic-field dependence of the lower-temperature peak. We find that the peak shows a sensitive dependence, which is highly contrasted to that of the Bonner-Fisher peak located in the higher-temperature region.[16] We think that this behavior is one of the key features for characterizing the fully frustrated spin systems. Therefore, the sensitive magnetic-field dependence may be observable in the experiment on the ^{3}He multilayer films if the double peak structure is a result of strong frustration effects as suggested by Elser and Zeng.[17]

This paper is organized as follows: Our numerical method for calculating the eigenvalue distribution functions is explained in Sec. II, in which the applicability of the procedure is examined through the numerical calculation on the 1D $S=\frac{1}{2}$ XY spin model (exactly solved model).[18] In Sec. III, the simulation results of the Δ-chain model are presented. For simplicity of the programming, we take advantage of only the total S^z as the quantum number of the subspaces; we treat up to 26-site systems in this paper. It is, however, possible to reduce the memory size by employing the other symmetry groups such as the space group; this programming effort obviously enables us to investigate larger system sizes than 26. A summary and discussions are given in Sec. IV.

II. METHODOLOGY

A. Numerical method

In general, the eigenvalue distribution function $\rho(\omega)$ may play a central role in describing the systems in various fields and the calculation of $\rho(\omega)$ is frequently the main substance of investigations:

$$\rho(\omega)=\mathrm{Tr}\,\delta(\omega-\mathcal{H})\ , \tag{1}$$

where $\mathcal{H}$ is the Hamiltonian of a certain system under consideration and "Tr" means the trace summation over a complete basis set. When a system possesses some conserved quantities such as the magnetization, the total number of particles, the total momentum, and the other quantities originating from a point group, the trace summation may be rewritten in the following form:

$$\rho(\omega)=\sum_{\mu}\rho_{\mu}(\omega)=\sum_{\mu}\mathrm{Tr}_{\mu}\delta(\omega-\mathcal{H})\ , \tag{2}$$

where μ denotes a set of the quantum numbers and Tr_{μ} is the trace over the basis set spanning the subspace defined by μ.

By writing the basis set as $\{|n;\mu\rangle: n=1,\ldots,\mathcal{N}_{\mu}\}$, we can express $\rho_{\mu}(\omega)$ in terms of Green's-function matrix elements:

$$\rho_{\mu}(\omega)=\sum_{n=1}^{\mathcal{N}_{\mu}}\rho_{\mu}(\omega,n)=\sum_{n=1}^{\mathcal{N}_{\mu}}-\frac{1}{\pi}\mathrm{Im}\mathcal{G}^{\mu}_{n,n}(z) \tag{3}$$

and

$$\mathcal{G}^{\mu}_{n,m}(z)=\left\langle n;\mu\left|\frac{1}{z-\mathcal{H}}\right|m;\mu\right\rangle\ , \tag{4}$$

where $z=\omega+i\epsilon$ and ϵ is a real positive infinitesimal. To calculate the diagonal elements of the Green's-function matrix, we introduce the recursion method, i.e., according to the Lanczos procedure, we create a new basis set using $|n;\mu\rangle$ as the initial vector, where the Hamiltonian has a tridiagonal representation:

$$[\mathbf{H}^{\mu}]_{k,h}=\begin{cases}\alpha^n_k, & k=h\\ \beta^n_k, & k=h-1\\ \beta^{n\,*}_h, & k=h+1\\ 0, & \text{otherwise}\ .\end{cases} \tag{5}$$

Then, $\mathcal{G}^{\mu}_{n,n}(z)$ can be expressed as a continued fraction form in terms of coefficients $\{\alpha^n_k,\beta^n_k\}$:

$$\mathcal{G}^{\mu}_{n,n}(z)=\cfrac{1}{z-\alpha^n_1-\cfrac{|\beta^n_1|^2}{z-\alpha^n_2-\cfrac{|\beta^n_2|^2}{\ddots}}}\ . \tag{6}$$

Previously, there have been some discussions about the termination of the continued fraction expansion;[13] some approximate terminators have been proposed. In our practical calculations, however, we adopt the truncation where the tridiagonal matrix elements are set to zero for $k>M$, because the truncation effects may be negligibly small when we use sufficiently large M. We will check the convergence of the calculated quantities against M (M is typically 50–200). Further, concerning the evaluation of the continued fractions, a simple "brute force" type calculation of $\mathrm{Im}[\mathcal{G}(\omega+i\epsilon)]$ is carried out with a finite ϵ, which imposes a Lorentzian broadening to the δ func-

tions contained in an eigenvalue distribution function. Thus, we should estimate the positions and the residues of poles contained in the smeared continuous function. The finite ϵ effects on the physical quantities are checked with the decrease of ϵ.

Our numerical approach may be reviewed as the generalization of the recursion method used in the electronic structure calculations, where the one-electron problem defined by the density functional theory is investigated in the real space to obtain the density of state.[13,19–22] For instance, corresponding to "the local density of state," one may consider $\rho_\mu(\omega,n)$ "the local eigenvalue distribution function," where the real space basis $\{|\mathbf{x}\rangle\}$ should be substituted by the complete basis set of a many-body system, i.e., $\{|n;\mu\rangle\}$. One important point is that once the recursion method is formulated, the treatment does not depend upon whether it is a one-body problem or not.

For a given initial state, e.g., $|n;\mu\rangle$, the computational effort of the Lanczos procedure scales as $\mathcal{N}_\mu$ for the systems with short-range interactions. This scaling property means that even when the memory size of a computer allows the calculations, the full trace summation in Eq. (3) is out of the CPU time limitation for larger size systems which scales as $\mathcal{N}_\mu^2$. Consequently, to relax the bottle neck of the $\mathcal{N}_\mu^2$ dependence, we should resort to a statistical treatment of the trace summation. For simplicity, we suppose that the Hamiltonian matrix is real symmetric; then except for the phase factor, an eigenstate of the Hamiltonian is expressed as the linear combination of a complete basis set with real coefficients, and thus, each normalized vector is represented by a point on the supersurface of the unit sphere in $\mathcal{N}_\mu$ dimensions. At this stage, we define the vector $|\Omega;\mu\rangle$ whose direction is Ω and consider the uniform integration of $\rho_\mu(\omega,\Omega)$ on the surface instead of the trace summation in Eq. (3). It is then clear that the integrated function is proportional to the eigenvalue distribution function:

$$\int d\Omega\,\rho_\mu(\omega,\Omega)\propto\rho_\mu(\omega)\ . \tag{7}$$

Therefore, we define our statistical treatment as the random sampling on the supersurface of the unit sphere in $\mathcal{N}_\mu$ dimensions. Finally, by normalizing the averaged function according to the sum rule:

$$\int_{-\infty}^{\infty} d\omega\,\rho_\mu(\omega)=\mathcal{N}_\mu\ , \tag{8}$$

and executing the summation over the subspaces, we can evaluate the total eigenvalue distribution function. It should be noted that in some cases, there is some other useful prior information about the distribution functions such as $\rho(\omega)=\rho(-\omega)$ and it may also be possible to take such information into the numerical calculation procedures, which are obviously expected to present rather small statistical errors for the calculated quantities.

Since Imada and Takahashi proposed a random sampling of the orthonormal basis in the quantum transfer Monte Carlo method,[12] similar techniques have been proposed and applied to the investigation of many-body properties of the quantum systems.[23,24] As was carefully discussed in Ref. 12, the strong self-averaging property is expected for the numerical calculation when using the above methods. In fact, as the system, i.e., $\mathcal{N}$, becomes large, the number of sampling vectors N_s can be reduced to evaluate the physical quantities within the same accuracy. In the following numerical calculations, we can also recognize this self-averaging property; we thus conclude that our sampling method efficiently contributes to relax the CPU time problem in the full trace summation.

B. Simulation results of the one-dimensional quantum XY model

In this subsection, we will show our calculation results on the 1D spin-$\frac{1}{2}$ quantum XY system with the periodic boundary condition:

$$\mathcal{H}_{XY}=2\sum_{l=1}^{N}(S_l^xS_{l+1}^x+S_l^yS_{l+1}^y)\ . \tag{9}$$

S_l^x and S_l^y are the components of the quantum spin on the lth site. The subspaces are classified by the total S^z and the systems up to $N=22$ are investigated. The number of sampling vectors N_s is a few thousands for smaller systems and several tens for larger ones. We divide the sampling vectors into typically five groups, and calculate "the short-time averages" for every group; the standard deviations of these averages are used to estimate the error bars of the calculated physical quantities. In the following discussions, we measure the temperature in units of $1/k_B$.

We first show the eigenvalue distribution function of the 10-site system in Fig. 2. This is an example of the histogram ($S^z=0$), which is compared with the exact data and exhibits a good agreement. In Fig. 3, the temperature dependence of the heat capacity $C(T)$ calculated from the eigenvalue distribution functions is presented with the exact result; we can also recognize the good agreement for the thermodynamic quantity. As an example of the system size dependence, we show the uniform magnetic susceptibility $\chi(T)$ at the low-temperature region in Fig. 4. The exact result in the thermodynamic

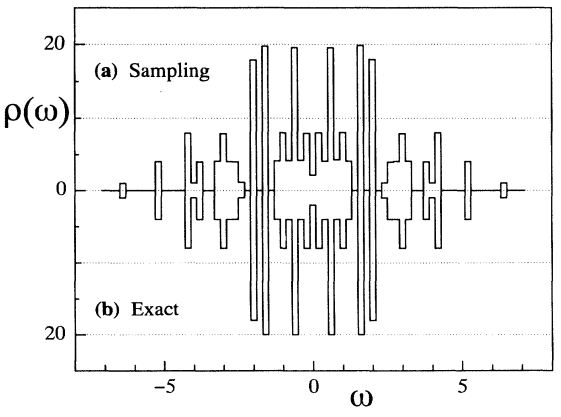

FIG. 2. The histogram of the eigenvalue distribution function of the 10-site XY spin system (the energy mesh $\delta\omega=0.2$): (a) sampling result, (b) exact result (we take the y axis downward). The number of sampling vectors $N_s=5000$. The data of the $S^z=0$ subspace is shown as an example.

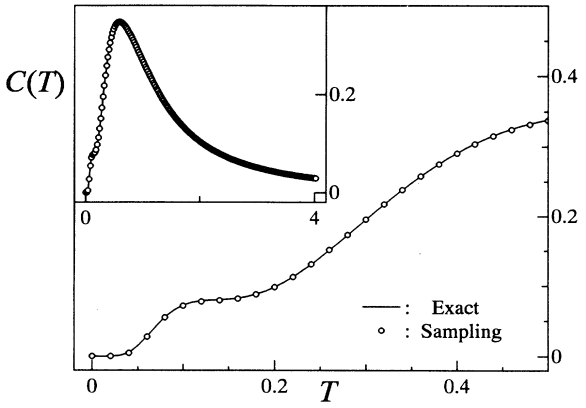

FIG. 3. The specific heat for the 1D 10-site XY spin system. The solid lines are the exact data and the open circles are the sampling ones. The inset shows the overall behavior.

limit is also presented as the solid line. We can see that the finite-size effects are decreasing with the increase of the system size; the numerical results reproduce the exact result accurately except for the lower-temperature region ($T \lesssim 0.1$).

The above simulation results enable us to conclude that our numerical calculation method efficiently works for the investigations of the many-body systems at finite temperature.

III. RESULTS

In this section, we present our numerical simulation results on the Δ-chain model under the uniform magnetic field $\mathbf{H}$ which is described by the Hamiltonian

$$\mathcal{H}=2\sum_{l=1}^{N}\mathbf{S}_l\cdot\mathbf{S}_{l+1}+2\sum_{l=1}^{N/2}\mathbf{S}_{2l-1}\cdot\mathbf{S}_{2l+1}-\sum_{l=1}^{N}\mathbf{H}\cdot\mathbf{S}_l\ . \tag{10}$$

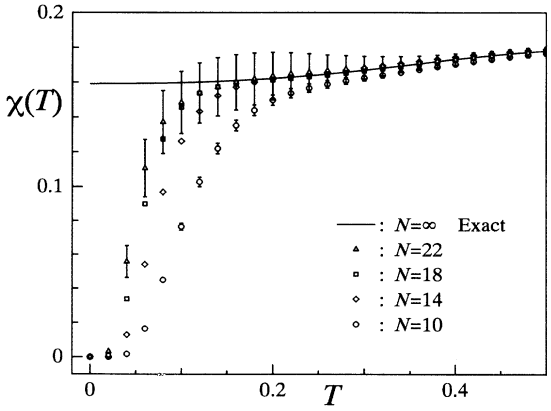

FIG. 4. The system size dependence of $\chi(T)$ data for the XY spin systems. The correspondence between symbols and the system sizes is shown. The exact result for the infinite system is drawn by the solid line.

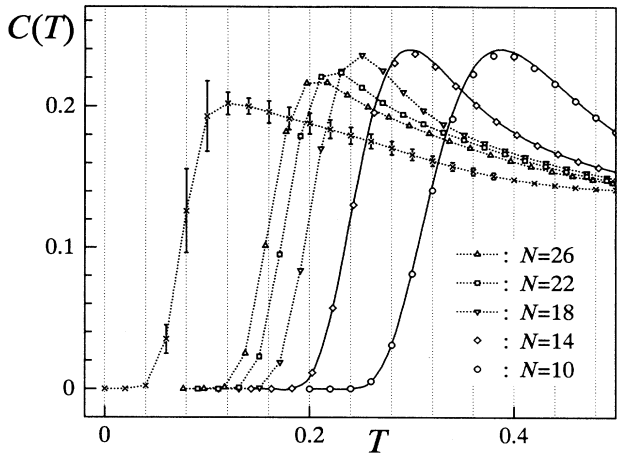

FIG. 5. The system size dependence of $C(T)$ for the Δ-chain model at the lower-temperature region. The original points are shifted rightwards according to $2/N$ for all system sizes data and the error bars are dropped. The cross ($\times$) shows the extrapolated results obtained from these size-dependent data. We also show the exact results for up to 14-site systems (solid lines).

The operator $\mathbf{S}_l$ denotes the quantum spin of size $\frac{1}{2}$ on the lth site. We employ the periodic boundary condition, i.e., $\mathbf{S}_{N+1}=\mathbf{S}_1$, and N is a certain even number. The first term is the Hamiltonian of the 1D antiferromagnetic Heisenberg model, which is known as the exactly solved model. The second term expresses the next-nearest-neighbor antiferromagnetic bonds, which introduce the full frustration effects into the Heisenberg antiferromagnet.

We start with showing the results at $H=|\mathbf{H}|=0$ in Figs. 5 and 6: the former plots the system size dependence of the specific-heat data and the latter is obtained by the extrapolation. The solid lines in Fig. 5 show the exact results for smaller systems (up to 14 sites) and the symbols denote our simulation data; the agreement may provide the reliability of our simulation results. We have

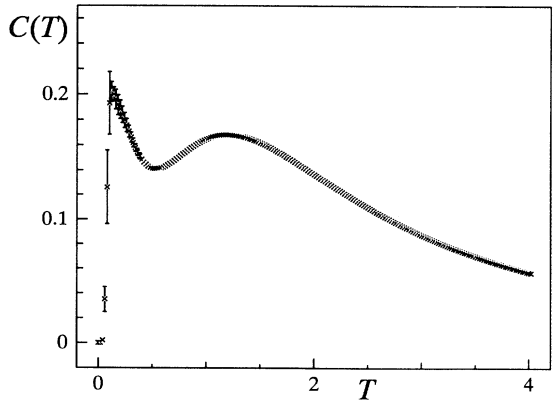

FIG. 6. The overall behavior of $C(T)$ for the Δ-chain model in the thermodynamic limit. The peak position $T_p \sim 0.12$ and the height $C_p \sim 0.2$.

also performed the same check for other physical quantities such as the uniform magnetic susceptibility. Although the system size dependence of the Bonner-Fisher peak[16] (the higher-temperature peak) is almost absent, it is observed in the lower-temperature peak, i.e., the height becomes lower and the position comes to locate at lower temperature with the increase of the system size. As a result, we estimate the peak position $T_p \simeq 0.12$ and the height $C_p \simeq 0.2$, respectively. The previous numerical study on this model had been carried out by using the quantum transfer-matrix method and the existence of the double peak structure is concluded.[6,25] As mentioned in that investigation, however, the low-temperature peak does not converge because of the insufficient Trotter numbers. On the other hand, our final result seems to coincide with the extrapolated values of those Trotter dependent data. We thus conclude that the double peak structure is confirmed quantitatively in the thermodynamic limit.

Next, we show the magnetization curve $m(H)$ of the Δ-chain model for various size systems in Fig. 7. The step functions expected for the ground states are smeared by the finite-temperature effect ($T=0.02$); however, the excitation gap can be estimated around $H_g \sim 0.43$; this agrees well with the previous exact diagonalization result indicated by the arrow.[6] To clarify the magnetic-field effects on the fully frustrated properties of the Δ-chain model, we should investigate the response from the excited states around the upper edge of the gap while keeping the ground state unchanged. For this aim, we restrict the magnetic-field strength as $H < H_g$.

We plot the magnetic-field dependence of the specific heat for the 26-site system in Fig. 8; the contrasted behavior of two peaks is clarified. With the increase of the magnetic field, the height of the lower-temperature peak becomes lower quickly and the width broader. On the other hand, the higher-temperature peak is hardly changed. The mean-field picture (coplanar order) predicts the fully frustrated effects as the simultaneous rotation of successive three spins, which gives rise to the high degeneracy of the states. It should be noted that this deformation is accompanied with the rotation of the local magnetization, so by applying the magnetic field, the energetically favorable orientation is realized. Corresponding to the above simple picture, the various spin states might degenerate around the upper edge of the excitation gap and the magnetic field should resolve the degeneracy according to their spin conditions. Consequently, we think that the change observed in the lower-temperature specific-heat peak is reflecting this magnetic-field effect.

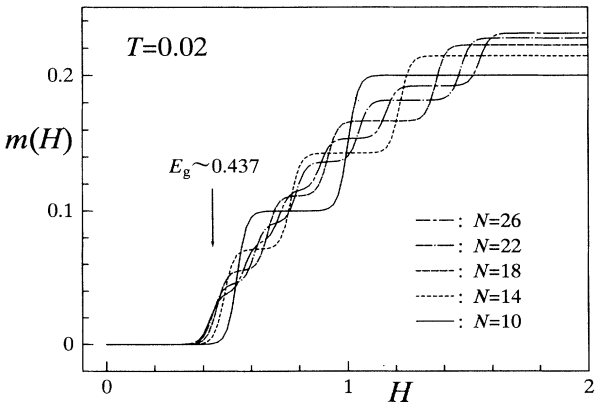

FIG. 7. The magnetization curves $m(H)$ for the Δ-chain model. The correspondence between line types and the system sizes is denoted. The temperature is fixed at $T=0.02$. The vertical arrow indicates the excitation gap E_g obtained by Kubo.

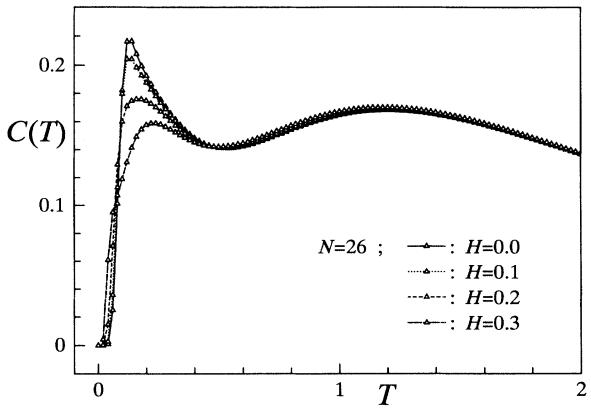

FIG. 8. The magnetic-field dependence of $C(T)$ for the 26-site Δ-chain model. The correspondence between the magnetic-field strength and the line types is denoted.

IV. SUMMARY

In this paper, the method to calculate the eigenvalue distribution function of a large scale matrix has been proposed, where the sampling procedure about random initial vectors is performed instead of the full trace summation of the imaginary part of the Green's function. The applicability of the method was examined through the numerical calculations on the 1D $S=\frac{1}{2}$ XY spin system; the feasible natures have been clarified. In particular, since our method exhibits a strong self-averaging property, accurate results are obtained by using a quite small number of sampling vectors for larger matrices.

By using the above method, we have investigated the Δ-chain model, where the magnetic-field effects on the lower-temperature peak observed in the specific-heat data were mainly discussed. The obtained results are summarized as follows. (1) The double peak structure of the specific heat is quantitatively obtained in the thermodynamic limit: we estimate the lower-temperature peak position $T_p \simeq 0.12$ and the height $C_p \simeq 0.2$ at $H=0$. (2) The lower-temperature peak exhibits a sensitive magnetic-field dependence—with the increase of the field, the peak becomes lower and broader quickly; it is highly contrasted against the Bonner-Fisher peak which is almost unchanged. The lower-temperature peak formation is thought to be a resultant of the high degeneracy of states due to the strong frustration effects. Further, the magnetic field may efficiently resolve the degeneracy,

which should be detected as the field dependence of the peak. We think the above observation exhibits one of the characteristic features of the strongly frustrated systems. Concerning the Heisenberg antiferromagnet on the *kagomé* lattice, the previously reported double peak structure is now thought to be a resultant of finite-size effects.[17,26] Therefore, our claim is as follows: the experimental measurement for the specific heat with the magnetic field may provide a significant insight into the question whether the low-temperature anomaly observed in the ^{3}He multilayer system has some relevance with the frustration.

Finally we notice that the applicability of our numerical calculation method is not restricted to the quantum spin systems. We also expect the method is efficiently applied to the correlated electron systems such as the high-T_c superconductors.

ACKNOWLEDGMENTS

The author is grateful to Professor Y. Okabe and Dr. T. Nishino for helpful discussions. Main computations were carried out on HP Apollo 9000 Model 735 at Tokyo Metropolitan University and NEC SX3 at Tohoku University. The present research was supported by a Grant-in-Aid for Scientific Research on Priority Areas "Computational Physics as a New Frontier in Condensed Matter Research," from the Ministry of Education, Science and Culture.

[1]H. Franco, R. E. Rapp, and H. Godfrin, Phys. Rev. Lett. **57**, 1161 (1986); D. S. Greywall, Phys. Rev. B **41**, 1842 (1990).
[2]X. Obradors *et al.*, Solid State Commun. **65**, 189 (1988).
[3]D. Huse and A. D. Rutenberg, Phys. Rev. B **45**, 7536 (1992).
[4]A. B. Harris, C. Kallin, and A. J. Berlinsky, Phys. Rev. B **45**, 2899 (1992).
[5]S. Sachdev, Phys. Rev. B **45**, 12 377 (1992).
[6]K. Kubo, Phys. Rev. B **48**, 10 552 (1993).
[7]F. Monti and A. Sütö, Phys. Lett. A **156**, 197 (1991).
[8]T. Hamada, J. Kane, S. Nakagawa, and Y. Natsume, J. Phys. Soc. Jpn. **57**, 1891 (1988).
[9]I. Harada, T. Kimura, and T. Tonegawa, J. Phys. Soc. Jpn. **57**, 2779 (1988).
[10]C. K. Majumdar and D. Ghosh, J. Math. Phys. **10**, 1388 (1969).
[11]T. Nakamura, N. Hatano, and H. Nishimori, J. Phys. Soc. Jpn. **61**, 3494 (1992).
[12]M. Imada and M. Takahashi, J. Phys. Soc. Jpn. **55**, 3354 (1986).
[13]R. Haydock, V. Heine, and M. J. Kelly, J. Phys. C **5**, 2845 (1972); **8**, 2591 (1975).
[14]H. Q. Lin and J. E. Gubernatis, Comput. Phys. **7**, 400 (1993).
[15]E. R. Gagliano and C. A. Balserio, Phys. Rev. Lett. **59**, 2999 (1987).
[16]J. C. Bonner and M. E. Fisher, Phys. Rev. **135**, A640 (1964).
[17]V. Elser, Phys. Rev. Lett. **62**, 2405 (1989); C. Zeng and V. Elser, Phys. Rev. B **42**, 8436 (1990).
[18]S. Katsura, Phys. Rev. **127**, 1508 (1962).
[19]S. Baroni and P. Giannozzi, Europhys. Lett. **17**, 547 (1992).
[20]W. Yang, Phys. Rev. Lett. **66**, 1438 (1991).
[21]G. Galli and M. Parrinello, Phys. Rev. Lett. **69**, 3547 (1992).
[22]D. A. Drabold and O. F. Sankey, Phys. Rev. Lett. **70**, 3631 (1993).
[23]J. Jaklič and P. Prelovšek, Phys. Rev. B **49**, 5065 (1993).
[24]F. Matsubara and S. Inawashiro, Solid State Commun. **67**, 229 (1988).
[25]S. Takada and K. Kubo, J. Phys. Soc. Jpn. **55**, 1671 (1986).
[26]K. Fukamachi and H. Nishimori, Phys. Rev. B **49**, 651 (1994).